Development of a Procedure to Compare Kinematics of Human Body Models for Pedestrian Simulations.

Corina Klug, Florian Feist, Marco Raffler, Wolfgang Sinz, Philippe Petit, James Ellway, Michiel van Ratingen

Abstract As Human Body Models are gaining increasingly relevance for the purpose of rating safety performance, it is essential that they behave consistently. Therefore, an objective method to compare human body models is needed. In this study a procedure to compare objectively human body kinematics was developed. Representative generic vehicle models were developed to simulate relevant pedestrian impacts. In a sensitivity study key boundary conditions influencing the head trajectory and contact time - such as the initial posture of the human body model or contact settings- were determined. Based on that findings a standardised procedure was developed and applied by propelling four generic vehicles at three impact velocities (30, 40 and 50 km/h) against two human body models (THUMS AM50 v4.02 and GHBMC M50 PS v1.4) in LS-Dyna. Trajectories of selected bony landmarks, head contact time and contact forces between the vehicle and the human body model were compared. Applying the developed procedure, the two human body models showed very comparable results in terms of trajectories and contact forces which gives the authors confidence in the robustness of the procedure developed and the models used.

Keywords Euro NCAP, human body models, pedestrian protection, harmonisation, pedestrian simulations, virtual testing

I. INTRODUCTION

Human Body Models (HBMs) are becoming increasingly important for the assessment of safety measures. They allow for evaluations of various human shapes and scenarios. Furthermore, they offer consideration of omnidirectional full body kinematics and analysis of enhanced output measures (e.g. strains).

The Euro NCAP (New Car Assessment Program) assessment of deployable systems (i.e. active bonnets) for pedestrian protection is the first application of HBMs in a consumer information rating.

Although human models can be used to estimate the injury risk to head, torso and lower extremities, such virtual injury measures are commonly not accepted by consumer rating programs. Consumers still expect their actual car to be tested and not a computer model only. On the other hand, some aspects of dynamic deploying systems can not be assessed with physical dummies as they are not humanlike enough or not available in various anthropometric sizes. By adopting a hybrid approach, Euro NCAP accepts that both methodologies could contribute to a robust assessment. The simulations with the pedestrian models are used to derive inputs for the subsequent physical assessment using conventional headform impactors. The virtual tests show the variety of scenarios that are addressed by the systems: First, the head impact location and Head Contact Time (HCT) for several pedestrian sizes is determined to assess if the system is fully deployed at the time of the head impact for the most critical pedestrian size. Based on that result, the bonnet is impacted with the head impactors in deployed or undeployed state (location dependent) in the physical test. Second, the for the sensor system hardest to detect pedestrian size can be determined by means of simulations as alternative to physical test and for the selection of appropriate test tools. Finally, the bonnet deflection due to the bonnet loading is derived to prove that the head protection is not compromised by a collapse of the bonnet. These simulations have to be carried out at varying impact speeds with several sizes of the pedestrian models (6YO, 5^{th}, 50^{th}, 95^{th}). [1]

C. Klug (corina.klug@tugraz.at, +43-316-873-30329) and M. Raffler are PhD Students, and. F. Feist and W. Sinz are Senior Scientists at the Vehicle Safety Institute of Graz University of Technology in Austria. Philippe Petit is Head of Research in Biomechanics at LAB PSA Peugeot-Citroën RENAULT (France). M. van Ratingen is Secretary General and J. Ellway Technical Manager at Euro NCAP (Belgium).

Human body modelling for crash simulations is an upcoming new field of expertise, which in recent years has evolved from purely research to more application based development at the vehicle manufacturer. Consequently, most vehicle manufacturers have highest confidence in their own in-house models, which may or may not be forked from more widely available HBMs. For the application of HBMs in ratings, it is essential that the results are comparable and reproducible. Currently, Euro NCAP accepts the results generated by various pedestrian models, as listed in the Technical Bulletin (TB) 13 [1], [2]. This approach, however, has led to an increasing number of accepted models, number of versions and models available in multiple codes, which raised the question whether all these alternative models would predict a similar outcome and lead to the same rating of the deployable system performance.

It is understood that the *biofidelity* of current HBMs is validated with several full scale and component level Post Mortem Human Subject (PMHS) tests [3–7]. At the moment, the data sources used for the validations vary between HBMs, which is shown exemplary in TABLE 1. Previous studies have also shown challenges for the translation of HBMs to different codes and highlight the importance of a harmonisation of HBMs for virtual testing [8, 9]. A certification procedure is needed, proving that different HBMs or a single HBM implemented in different codes behave consistently. However, up to now, no objective standardised comparison method of the response of various HBMs in multiple codes, i.e. independent of the HBM and FE code, is available. Furthermore, several studies show that kinematics of HBMs is sensitive to initial conditions like posture or friction between pedestrian and vehicle [4, 10–15]. But some of these boundary conditions are only prescribed in broad terms in the current version of the Euro NCAP pedestrian testing protocol [1].

TABLE 1:
EXAMPLES FOR VALIDATION OF THUMS V4 AND GHBMC PEDESTRIAN MODEL [3–7]

	Full Body Trajectories	**Knee**	**Lumbar Spine**
GHBMC	Kerrigan et al., 2007 [16]	Bose et al., 2008 [17]	Rohlmann et al, 2001 [18]
THUMS	Subit et al. 2008, [19] Schroeder et al., 2008 [20] Forman at al., 2015 [21, 22]	Bose et al., 2004 [23]; Kajzer et al., 1997 [24]	Demetropoulos et al. 1998 [25]

The current study aims to be a first step towards a certification procedure of pedestrian models. Such a procedure shall ensure that all CAE pedestrian models which can be used for the Euro NCAP rating behave consistently and lead to comparable results. While it is clear that the introduction of such procedure would improve the confidence in the results obtained from the vehicle manufacturers, it also avoids that only one type of HBM in one code would be accepted for virtual testing by Euro NCAP in the future.

A procedure is developed which enables the objective comparison of HBM kinematics for representative pedestrian loadcases. The protocol summarises and standardises boundary conditions which have to be considered and consistent to enable a fair comparison between simulation results.

The following research questions were investigated within the current study:

- How can the structural behaviour of a car front be modelled in a representative and very simplified way?
- Which boundary conditions and simulation settings are affecting the trajectories, head contact time and contact forces and therefore have to be defined for a proper protocol for pedestrian simulations?
- What is the effect of modified boundary conditions compared to the difference induced by the use of different HBMs?
- Do simulations with two different HBMs lead to comparable results in terms of kinematics (relevant for the Euro NCAP assessment of deployable systems), when consistent boundary conditions are applied?

II. METHODS

A simulation setup for the comparison of HBMs was defined consisting of the following requisites:

- Establishment of generic vehicle models representative of contemporary passenger cars

- Definition of nodes for tracking HBM kinematics
- Definition of initial HBM posture
- Definition of contact settings
- Definition of post processing

Within a sensitivity study boundary conditions which affect the HBM kinematics were identified in order to move ahead with the development of a robust procedure. Subsequently, the standardized procedure as developed was applied to the two HBMs. The 50th percentile male Total Human Model of Safety (THUMS) v4.02 and the simplified Global Human Body Models Consortium (GHBMC) v1-4 pedestrian models were used in the study in LS-Dyna (Livermore Software Technology Corporation, USA). All simulations were performed with the LS-Dyna R7.1.1. (mpp version redhat54_ifort131_sse2_openmpi165).

To comply with the current Euro NCAP protocol [1], the following boundary conditions were applied to all simulations:

- the heel to heel distance was 310 ± 10 mm
- the head centre of gravity (COG) was aligned with the vehicle centreline
- the struck side leg was facing backwards
- the coefficient of friction between the HBM and the ground was set to 0.3

Representative Generic Vehicle Models

Three dimensional median geometries have been established as a means of deriving representative vehicle shapes: the vehicle geometries of current European cars were parameterised based on outer shapes provided by car manufactures or pictures with vehicle dimensions. The vehicle midsection consists of ten Bézier curves shown in Fig. 1. Start- and endpoint and corresponding slope of the tangents are defined for every single curve. The whole vehicle front was described with 120 parameters. The median value for each parameter was derived for each vehicle category resulting in representative median vehicle shapes for four different vehicle categories: Sport Utility Vehicle (SUV), Family Car/Sedan (FC), Roadster (RDS) and Multi-purpose vehicles and Superminis (MPV).

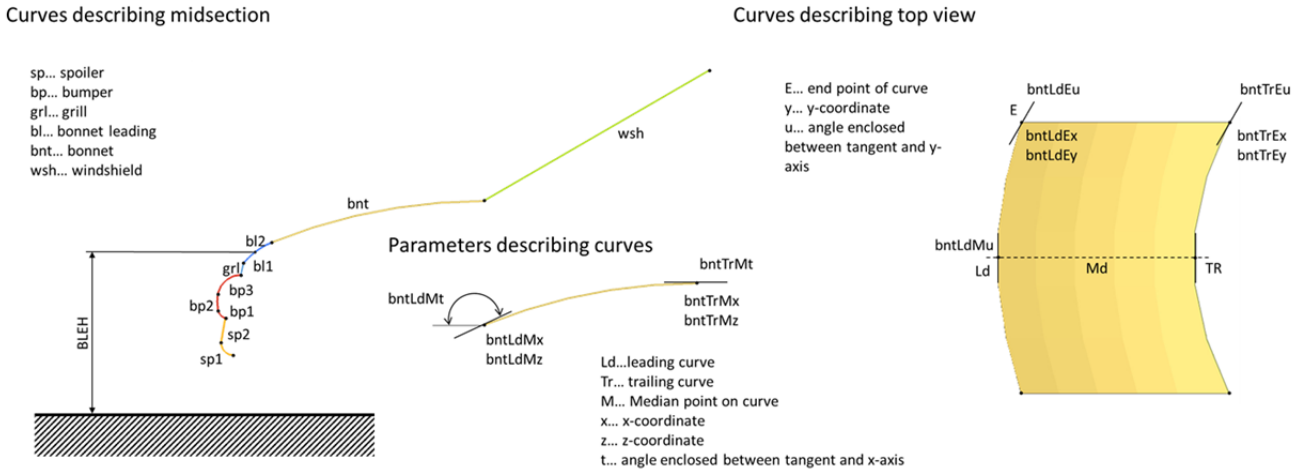

Fig. 1: Parameters of Bézier curves defining the vehicle geometry

A modelling approach was chosen, which is easily transferable to other finite element (FE) codes (Radioss, Pam-Crash and Abaqus) as simple material models are used. The generic vehicle (GV) model structure is shown in Fig. 2. It was assumed that the structural response under the loads of a pedestrian impact can be modelled through an outer shell surface, an interface layer (for modelling the vehicles fascia), and a generic foam, the foam layer, resting on a rigid skeletal vehicle structure, the bottom layer. The compaction layer emulates hard structures and works as an end stop, as a contact with the interface layer is defined. The foam is intended to replicate a variety of unknown base structures, such as for example ribs, collapsible cones, buckling structures and foams, i.e. structures which absorb energy. It features piecewise-linear behaviour, defined energy absorption, negligible expansion under compression and no strain rate dependency. In LS-Dyna the Mat_Fu_Chang_Foam with log-log interpolation was used (with one unloading curve and two equivalent

loading curves). To prevent any issues associated with spurious modes (hourglassing) and issues with volume-locking, the foam layer was assigned selective-reduced integration (SRI) hexaeder elements. The surface of the foam was covered by an interface layer, which provides a realistic mass of the contact interface and thus inertial effects upon impact and realistic structural mechanical characteristics (Young's modulus, Tangential modulus, yield stress of steel for the bonnet and plastic for the other parts).

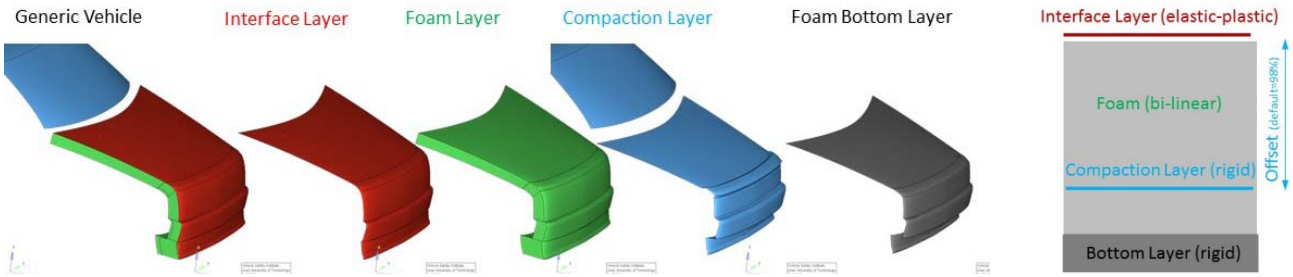

Fig. 2: Layers forming the GV models.

The software LS-Opt was used to calibrate the material parameters of the foam and the thickness of the interface layer to a representative structural behaviour.

The target curves for the *representative structural behaviour* were derived from impactor simulations run with state of the art FE vehicle models of current European cars, which were validated for pedestrian protection tests. A rigid cylindrical impactor with a total mass of 5.95 kg (density= 7,89E-6 kg/mm³, diameter= 120 mm, height= 400 mm and wall thickness= 5 mm) was propelled against eight locations on the spoiler, bumper, bonnet lead and bonnet once at the vehicle centreline (CL) and once at the location of the bumper corner (BC), the definition according to Euro NCAP pedestrian protocol v8.2. No physical tests have been performed. A rigid impactor was used to avoid deformations of the impactor and therefore simplify the optimization of the material parameters of the generic vehicle (GV) model. The median force for each deflection step was calculated at first for each vehicle category. The median mass (median kerb weight of the vehicle and the additional mass of 150 kg for driver and front passenger as specified in the Euro NCAP pedestrian testing protocol), as established for each vehicle category, was assigned to the vehicle model. However, the vehicle's moments of inertia remain unconsidered, as the vehicles have only one degree of freedom, which is the x-direction in the vehicle coordinate system.

Definition of Sensors for Tracking HBM Kinematics

For the evaluation of trajectories, *sensors* were implemented in the HBMs at selected structural points: The head centre of gravity (HC), the centre (average of all nodal coordinates) of the vertebrae C1, C7 and T12, the nodal midpoint of the left and right centre of the acetabulum (AC), the inter-malleolar point on the right (MR) and left leg (ML) and the centre of the right (KR) and left patella (KL).

The sensors were connected with the surrounding structure by interpolation constraints (Keyword *CONSTRAINT_INTERPOLATION in LS-DYNA), so that the motion of the single node used as sensor depends on the averaged motion of a set of master (independent) nodes. Comparable approaches are available in all codes: OTMCO in VPS, RBE3 in RADIOSS and Distributing coupling in Abaqus.

Definition of Initial HBM Posture

Key parameters of the initial posture of the HBM affecting the kinematics in pedestrian simulations were identified by means of a sensitivity study. THUMS was repositioned by carrying out pre-simulations. The GHBMC model was geometrically repositioned by elemance (USA) to match the THUMS position as closely as possible. Eleven different postures were defined, and each of these is specified in Table AVI in the Appendix. The defined postures are based on [26], the posture defined by [27, 28] (40% gait cycle) and the position of the pedestrian target used for the AEB (Autonomous Emergency Breaking) testing [29].

The posture of the arms, torso angle, leg angle, shoe angle and the head angle were slightly varied to analyse the sensitivity respectively. Only the posture of the arms was varied for the GHBMC. The angles were measured based on anatomic landmarks taking into account the recommended landmarks for anatomic axis definitions

from the international society of biomechanics [30, 31]. The femur reference axis was defined as the connection between the centre of the nodes of the acetabulum and the midpoint (FE_right/left) between Epicondylus femoralis medialis (FEM) and Epicondylus femoralis lateralis (FEL). The knee flexion angle was measured between the femur reference axis and the connection between FE_rigth/left and the inter-malleolar point (M_right/left), which is located midway between the tip of the medial malleolus (MM) and tip of the lateral malleolus (LM). The humerus reference axis was defined as the connection between the midpoint (hereafter called SC_right/left) of the most laterodorsal point of Angulus Acromialis (AA) and the most ventral point of Processus coracoideus (PC) and the midpoint (HM_right/left of the most caudal point on the lateral epicondyle (EL) and the most caudal point on medial epicondyle (EM). The Elbow Flexion Angle was defined as the angle between the humerus reference axis and the connection between HM and the most caudal-medial point on the ulnar styloid (US_right/left).

The sensitivity study was carried out using the generic family car with an impact velocity of 40 km/h. To prove if the conclusions can be transferred to other loadcases selected variations have also been simulated with the generic SUV model.

Definition of other Simulation Settings

Impact velocities must be in the range relevant for the subsequent Euro NCAP rating which is from 30 to 50 km/h. The sensitivity study was carried out for the impact with the generic family car model at an impact velocity of 40 km/h. A gravity field was applied in all simulations.

Variations of the contact between the vehicle and the HBMs were performed: For the baseline simulations a segment-based contact (SOFT=2, DEPTH=13) with a coefficient of friction (FS and FD) of 0.3 and a viscous damping coefficient (VDC) of 20% was defined. A variation of the damping coefficient (VDC=0), coefficient of friction (fric=0.2-0.5) and a change to the default penalty formulation (SOFT=0, DEPTH=2) was performed. Furthermore, the effect of pre-simulations was analysed (until the vertical force between the ground and the HBM was equal to the HBM's weight force) and the coefficient of friction between the HBM and the ground (0.3-0.9) was investigated.

Definition of Post Processing

The global coordinate system was defined at t0 as the x-direction parallel to the vehicle longitudinal axis in driving direction and the z-direction parallel to the vehicle height axis facing upwards. For the evaluation of the trajectories the x displacement of the vehicle was subtracted from the x-coordinates of the sensors (stationary vehicle view). Contact forces and node histories were output every 0.1 ms. Unfiltered curves were used.

The head contact time (HCT) was defined as the time from the first increase of the bumper contact force (C) until the first increase of the resultant head acceleration where it reaches its maximum (H). If this was not clearly identifiable, the contact force between the vehicle and the head was used additionally (first time when contact force is not zero anymore). An example of the definition of HCT is shown in Fig. 3.

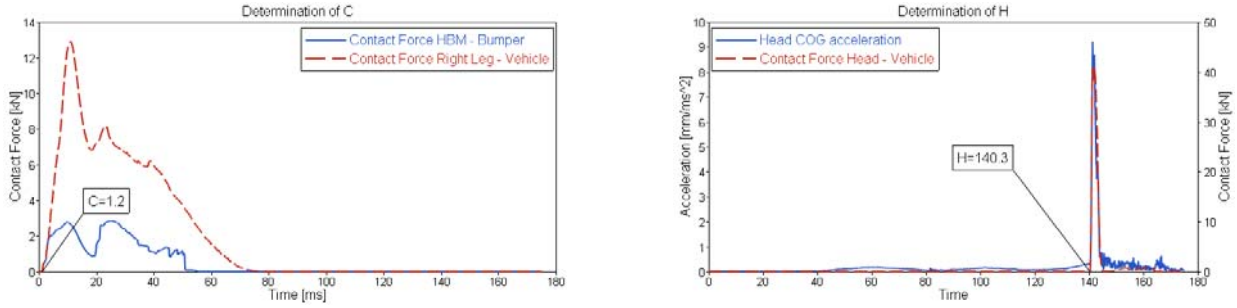

Fig. 3: Determination of Head Contact Time HCT= H-C.

Application of Final Procedure

Eventually all relevant boundary conditions were fixed and set equally for simulations with THUMS and GHBMC. Posture 3 was chosen as final reference posture, which is a combination of the leg posture defined in [26] and a natural arm posture [27]. Both models were impacted with all four different vehicle models at three different impact velocities and results of the two models were compared.

III. RESULTS

Representative Generic Vehicle Models

Four representative GV models were developed. Fig. 4 shows the finalised GV models. The midsection of the vehicle geometries is shown in Fig. 5 and compared to current European vehicles in Fig. A1. The GV was separated into the deformable areas Spoiler (spl), Bumper (bmp), Grill (grl), Bonnet Lead (ble), Bonnet (bnt). A rigid surface was used for modelling the windscreen and the roof as these areas were irrelevant for the current study.

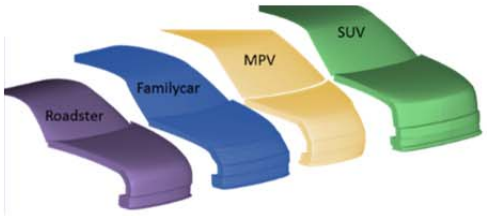

Fig. 4: Generic Vehicle Models.

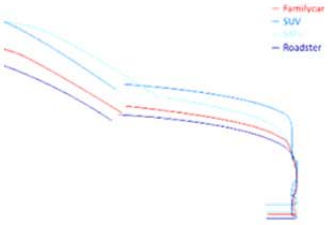

Fig. 5: Midsection of vehicle geometries.

Fig. 6: Loadcases at vehicle centerline.

In total, 11 vehicle models from five different car manufacturers were used for deriving the stiffness corridors. Force-Deflection curves, as shown in Fig. 7 for the impact at the bumper centreline were discretised (2.5 mm steps) and separated into loading and unloading curves.

As shown in Fig. 8, differences of the median force deflection curves for differing vehicle categories were observed to be smaller than differences within one vehicle category. Hence, median curves were derived from all 11 vehicles (over all categories). Corridors were defined from the minimum force to the maximum force for each deflection from the responses of all full FE vehicles. One corridor and median curve was established per load case which can be used for all vehicle categories. It was observed, that roadsters showed less clearance in the bonnet impacts, which was considered for the modelling of the GV by setting the offset between compaction layer and interface layer to 68 instead of 99 (which was used for the other geometries). In Fig. 6 the deformations of the GV, the family car, for all load cases at the vehicle centreline are shown. Fig. 9 shows the final response of the generic family car model in LS-DYNA for the impact with the rigid impactor at the bumper centreline with the final parameters derived from the optimisation. The results of all load cases and all vehicle geometries together with the corridors and the final parameters are included in the Appendix.

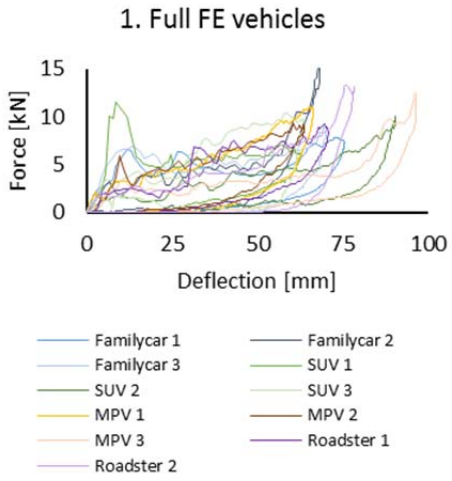

Fig. 7: Force deflection characteristic of single vehicles for impact simulations at bumper centreline.

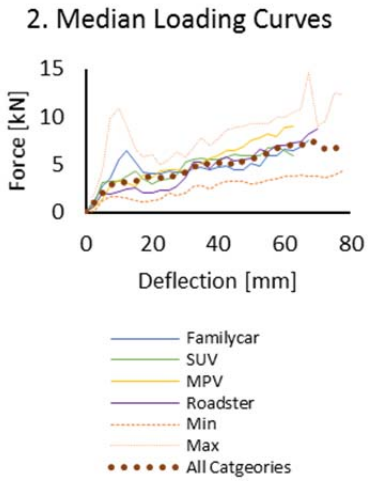

Fig. 8: Median Loading Curves for impact at bumper centreline for single vehicle categories and over all categories.

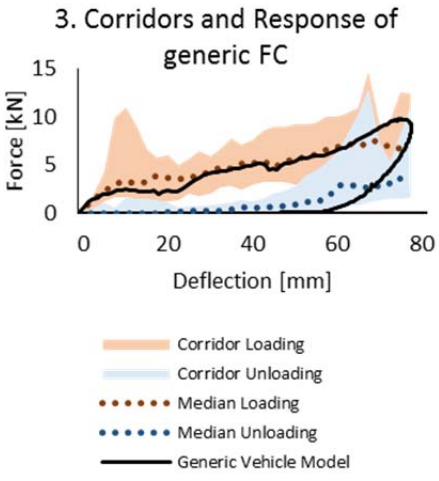

Fig. 9: Response of generic family car model in LS-DYNA compared to corridors and median curve for loading and loading (impact at bumper centreline).

Definition of Initial HBM Posture

Fig. 10 shows the repositioned THUMS in all analysed postures. The variation of the arm posture for GHBMC is shown in Fig. 11. For Postures 1, 2 and 3 only the posture of the arms was varied. Posture 4 has slightly changed arms and legs. Postures 5, 6, 10 and 11 show a variation of torso and/or neck angle and therefore varying head positions (HC). For Posture 7 and 8 the sole angle was modified from Posture 2 and 3, respectively. Posture 9 shows the same arm posture as Posture 3, but a slightly modified leg posture.

The maximum difference of the head contact time due to a variation of the initial posture for THUMS was 3.7 ms (Fig. 12). For GHBMC the modification of the arm posture led to a difference in HCT of up to 5.2 ms (Fig. 13).

Within the THUMS simulations, just changing the posture of the arms led to a variation in head contact time of up to 1.8 ms (when arms were positioned in front of the pedestrian compared to a natural posture). The angle of the shoes was changed for Postures 7 and 8, which resulted in a higher position of the acetabulum and the head. The 15 mm higher initial position of HC and AC led to a 1.3 ms higher head contact time for arm posture 2 and 1.2 ms for arm posture 3. Changing only the x and z position of HC led to a difference in HCT of 1.4 ms. A modification of the torso angle (C7x) resulting in a 13 mm smaller z-positon of HC did not cause a difference in HCT when the x-position of HC remained unchanged (Posture 10 compared to Posture 11).

By contrast, Posture 4 shows the same height of AC and HC as Posture 1, 2 or 3 and only a small modification of the arm and leg angles, but causes a significantly smaller HCT. A pure modification of the leg posture led to virtually no difference in HCT (ΔHCT of Pos 9 and Pos 3 is only 0.2 ms).

Differences of the second peak of the contact forces (at about 30 ms) were found when the posture of the legs was modified (Fig. 15).

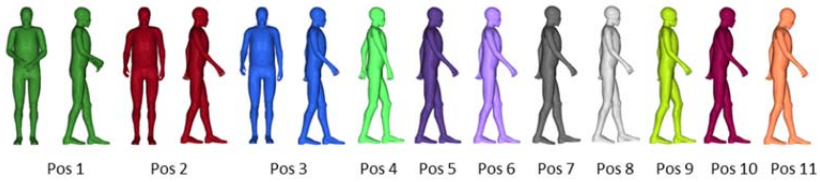

Fig. 10: THUMS postures.

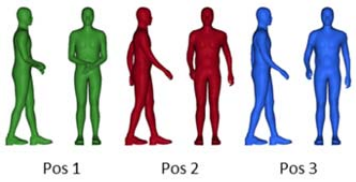

Fig. 11: GHBMC initial postures.

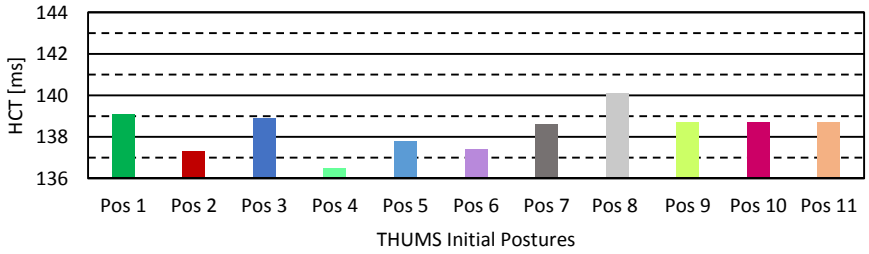

Fig. 12: Influence of initial posture of THUMS on HCT.

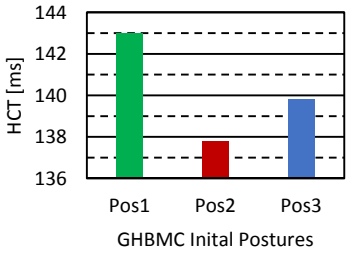

Fig. 13: Influence of initial posture of GHBMC on HCT.

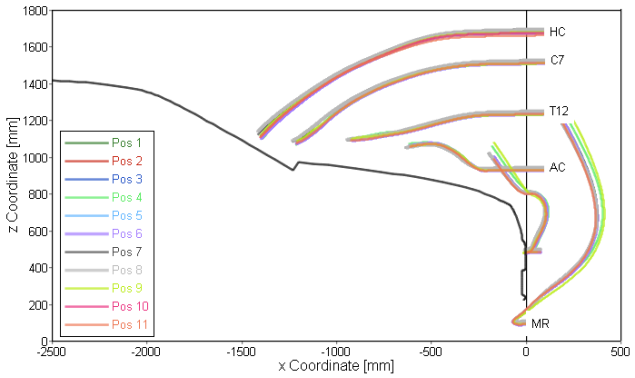

Fig. 14: Influence of initial posture of THUMS on trajectories
(impact with generic family car model at 40 km/h).

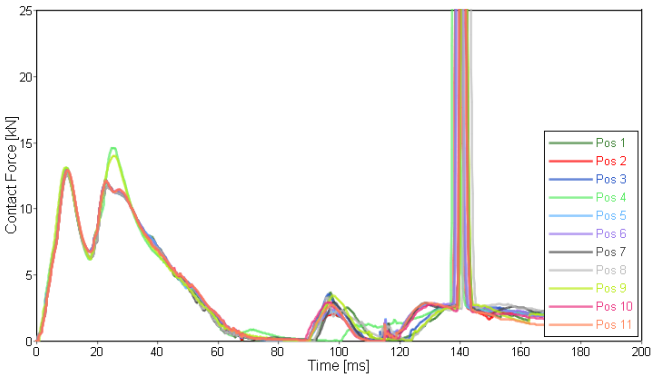

Fig. 15: Influence of initial posture of THUMS on total contact forces (impact with generic family car model at 40 km/h).

No great differences in the trajectories were observed due to modifications of the initial posture of the HBMs as shown in Fig. 14. The position of the arms has negligable effect on the trajectories of the THUMS and GHBMC, which is shown in Fig. 16. To prove this conclusion, simulations with the generic SUV model at 40 km/h were performed with THUMS in Posture 1, 2 and 3. No influence of the initial posture on the trajectories was observed for this loadcase as well (Fig. A2 and A3 in the Appendix).

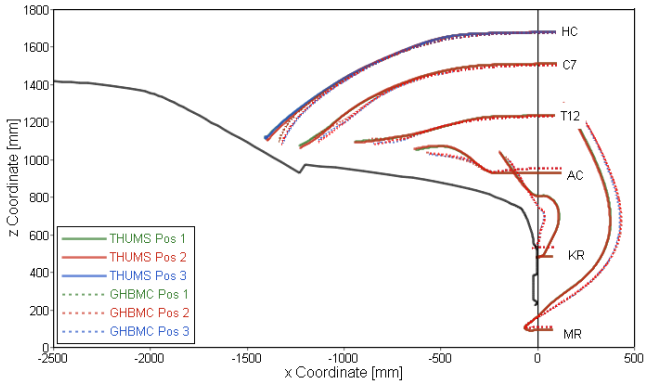

Fig. 16: Influence of initial arm posture on trajectories (impact with generic FC model at 40 km/h)

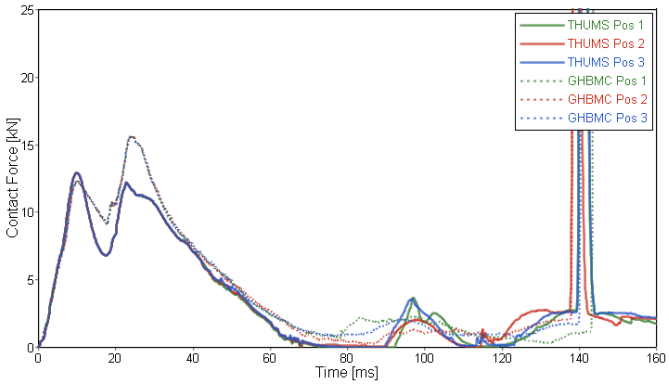

Fig. 17: Influence of initial arm posture on total contact forces.
(impact with generic FC model at 40 km/h)

The same trend was observed for both HBMs: Posture 1 led to the highest and Posture 2 to the smallest HCT. Differences in the support provided by the arm were observed leading to a divergence especially in the z velocity of the head COG. The contact forces are showing some differences as soon as the ellbow is contacting the bonnet of the vehicle (Fig. 17). The observed contact force between the right arm of THUMS and the bonnet was only 2 kN for Posture 2 while it was 3.7 kN for Posture 3 and 3.5 kN for Posture 1.

Fig 18 shows the differing angles of the humerus for the simulations with GHBMC with initial Postures 1, 2 and 3 and the corresponding head velocities in the global coordinate system. The difference of the resultant head impact velocity at the time of head contact was 0.7 m/s and the maximum difference of the resultant velocity at the same time (140 ms – HCT of Posture 2) was 1.5 m/s .

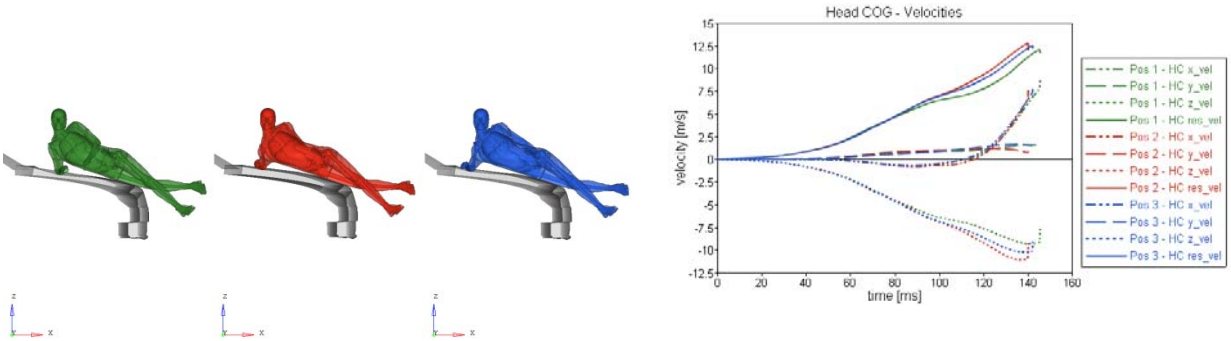

Fig 18.: Support of humerus for Posture 1 (left) and 3 (right) at 100 ms (FC with 40 km/h, GHBMC).

As the difference between the two models in terms of HCT was smallest for Posture 3 and the posture represents a natural walking position [27], this posture was used as baseline for the following simulations. Fig. 19 shows THUMS and GHBMC in Posture 3. In the right figure the two models are overlaid, showing that the postures match very well.

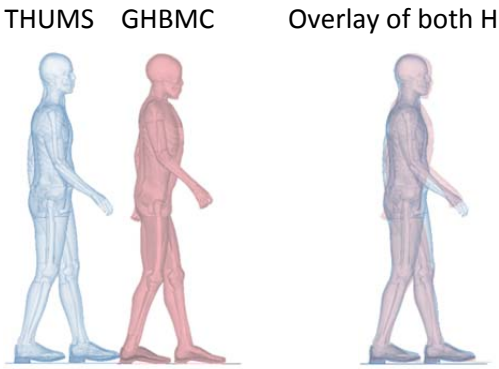

Fig. 19: Geometrical comparison of THUMS (blue) and GHBMC (red) in Posture 3

Definition of Simulation Settings

The trajectories and head contact time were found to be sensitive to the contact setting (Fig. 20) Changing the contact algorithm from segment-based (checks for segment vs. segment) to default (node to segment) lead to a higher head impact point (58 mm difference in the x-z plane) and a 2.3 ms higher head contact time. The node to segment formulation led partly to penetrations of the HBM outer surface into the interface layer of the GV. Therefore, the segment to segment formulation is preferable. Increasing the friction between the vehicle and the pedestrian led to a decrease of HCT (Fig. 21) and a lower endpoint of the head trajectory (Fig. 20). A modfication of the damping coefficient VDC had no effect on HCT or the trajectories.

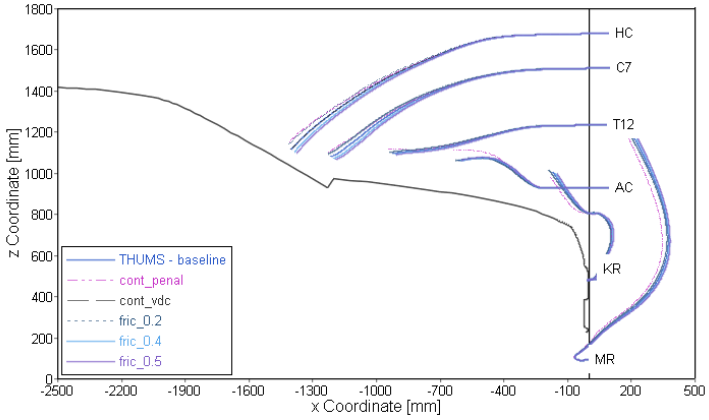

Fig. 20: Sensitivity of Trajectories to modifications of contact options with THUMS (impact with generic family car model at 40 km/h).

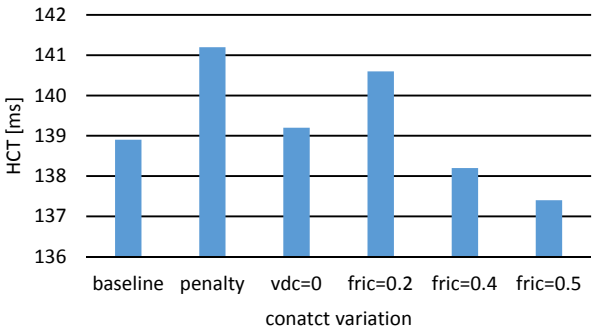

Fig. 21. Sensitivity of HCT to modifications of contact options (THUMS impact with generic family car model at 40 km/h).

Application of Final Procedure

Based on the results of the sensitivity study the following boundary conditions were fixed for the final procedure (and discussed within Chapter IV):

- The HBMs were used in Posture 3
- The segment based contact algorithm was used
- The coefficient of friction between the vehicle and the HBM was fixed to 0.3
- No presimulations were performed

Both HBMs were impacted at 30, 40 and 50 km/h with the four GV models. Contact forces, HCT and trajectories of the two models were compared. All results are shown in Table AV in the Appendix. The maximum difference of HCT was 3.5 ms and was observed at the impact with the SUV at 40 km/h. The average difference in HCT was 1.9 ms (in 7 of the 12 simulations the difference was smaller than 2 ms). The best correlation was observed for the impacts with the family car (mean ΔHCT=1 ms). The largest difference in terms of trajectories was observed for the impact with the roadster at 30 km/h (Fig. 22). The distance between the locations of HC of

the two models was 143 mm. The difference in HCT was 0.6 ms, which was the smallest value in all the simulations. The contact forces of the two models were very similar for all impact cases. Only very minor differences of the first peak (leg impact) between the two models have been found. Some differences were observed for the second peak and the unloading (hip impact at the bonnet leading edge) an example of which is shown in Fig. 23. Some difference in the timing of the contact of the arms with the bonnet is also shown here.

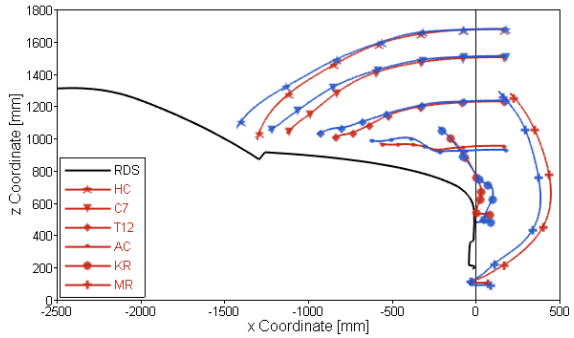

Fig. 22: Comparison of trajectories of THUMS (blue) and GHBMC (red) for the impact with the generic roadster model at 30 km/h.

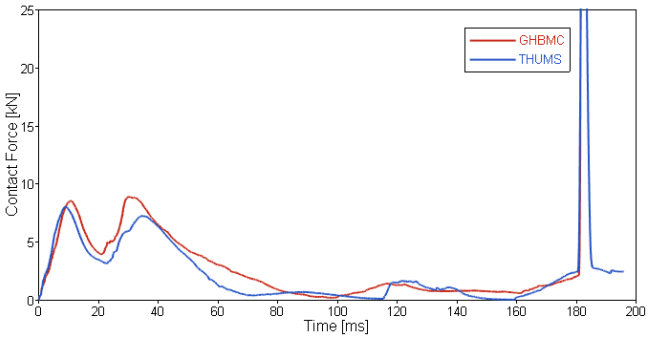

Fig. 23: Comparison of contact forces of THUMS and GHBMC for the impact with the generic roadster model at 30 km/h.

IV. DISCUSSION

Representative Generic Vehicle Models

Approx. 10 years ago in the project APROSYS (Advanced Protection Systems) stiffness corridors for the bumper, the bonnet leading edge, the bonnet and the windscreen of the European fleet have been derived from Euro NCAP results. The current study aimed to re-examine the structural behaviour for the contemporary European fleet.

Results of eleven full FE vehicle models have been available to gain the force deflection characteristic for the current study. As the differences between the categories were found to be smaller than the differences within one category, the median from all 11 vehicles was calculated.

As the difference between the various categories were found to be very small the median from all 11 vehicles was calculated which avoids to use medians which are based on three vehicle models only. The results of the current study were compared with results and applied stiffnesses from previous studies.

The resulting stiffness values of the current study compared to other studies are shown in Fig.24. While the stiffness of the bumper matches the green characteristic derived by [32] and the stiffness used by [33], differences of for the spoiler and the bonnet leading edge are considerable. This might be caused by the different methodology and design changes over the last 10 years.

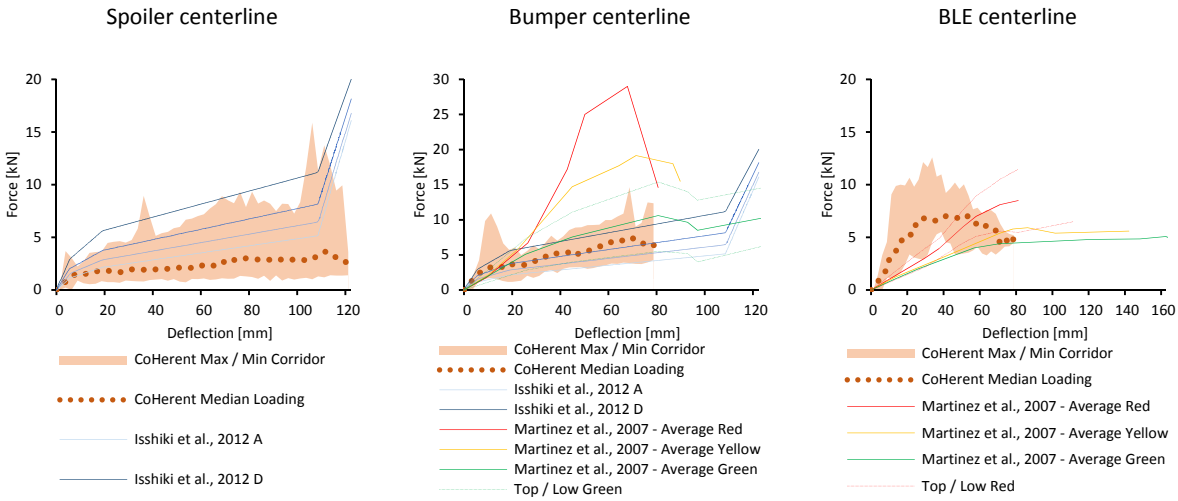

Fig.24: Comparison of representative vehicle stiffness of the current study and studies of [32, 33]

A very simplified approach for modelling deriving the structural behaviour was used to rule out any influence by the impactor and to maximize as the robustness and transferability to other codes. For future applications focusing on injury measures of the HBM instead of pure kinematics the vehicle models should be further validated by comparing injury measures of HBM simulations with full FE vehicle models impacting HBMs.

Definition of Sensors for Tracking HBM Kinematics

The center of all nodes was chosen as this definition is easily applicable and robust. It was easy to identify the proposed locations in both HBMs and the location of the sensors was repeatable. Several trials led to very similar results with differences smaller than the average element size of the HBMS. To check plausibility of this approach as well as the effect of the mesh size a simple example was used: A sphere with 100 mm radius was meshed with varying element sizes (20-2.5mm) and the location of the center of all nodes was compared. The maximum difference to the center of the surface was 5.4 mm for the 20 mm element size (so ¼ of the element size and less than 3% of the diameter of the sphere).

Definition of Initial HBM Posture

Several studies indicated that the initial pedestrian stance is affecting the impact kinematics [11, 14, 34]. In real world a variety of impact scenarios and pre-crash reactions of the pedestrian [35] can happen. Anyway, the car manufactures need design targets. Therefore, the definition of position(s) is important to enable the comparability of virtual testing results. For the future it could be beneficial to perform assessment simulations in various predefined initial positions to cover more real world scenarios, but for the moment only one positon was chosen. An open source positioning tool like it was developed within the PIPER (Position and Personalize Advanced Human Body Models for Injury Prediction) project [36] could be used in the future to further specify the initial posture, avoid errors, or finally even the positioning procedure.

All postures used within this study are replications of a midstance. This is in accordance with [13] who propose to use the midstance because it is most representative for pedestrian collisions and represents a “significant proportion of the normal gait (16-22%)”.

Within the Euro NCAP pedestrian protocol [1] it is defined that the struck side leg should face backwords. This stance represents the “worst case”, as [14] shows that head impact velocities and WAD are smaller for impacts with the struck side leg facing forwards, as this stance tends to cause more lateral displacement of the pedestrian.

The position of the arms was completely open in the current version of the Euro NCAP pedestrian testing protocol. Therefore, the initial posture of the arms was highly varying within the simulations performed by the car manufactures reported to Euro NCAP. Some studies are available showing that the posture of the arms is affecting the torso and head kinematics [37–40]. The effect is often caused by the comparison of no support of the arms to the bonnet (wrists tied together or arm gets pinned between the thorax and the vehicle) versus supporting arms [37]. Within the current study the arms of the HBMs were always supporting on the bonnet. No effect of the varying arm postures was observed for the variations of the arm postures, but the highest difference of head contact time between the two HBMs was observed for variation of the arms. It should be mentioned that the modifications of the arm posture were more extensive than the repositioning of the legs, when comparing Posture 1 to 2. But also the slight modification between Posture 2 and 3 caused 2 ms differences in HCT. It was surprising that posture 2 and 3 led to such big differences in HCT although they look visually alike. The struck side arm of posture 2 was less loaded. It seems that the higher the contact forces between the arm and the bonnet, the larger the head contact time (when legs and torso are positioned consistently), as the increasing support of the arm decreases the velocity of the head and torso, which is in accordance with the findings of [41].

When analysing the trajectories relative to the vehicle they look nearly congruent in the figures. The distance of the location of HC from the simulations with posture 2 and posture 3 at the time of head impact relative to the vehicle is 11 mm. In the x-z-plane the max. spatial difference between trajectories amounts for 5 mm. At 130 ms the max. difference of the x-positon of HC can be observed (5.5 mm). The head of posture 2 is 20 mm lower than of the other postures at that time. Small spatial differences of the location of the head can already lead to differences in HCT of some milliseconds, as the vehicle is moving with 11 mm/ms.

It has to be mentioned that the lack of knowledge on the biofidelity of the arm kinematics could be one limitation. Except from the study of [12], no validation of the arm kinematics on a full scale level has been performed. In PMHS tests the wrists of the subjects are usually tied together to gain better repeatability [16, 19, 21]. This is proposed to avoid that the arm of the PMHS is being pinned between the thorax and the vehicle [13].

It was shown that the height of the acetabulum centre was affecting HCT, which is in accordance with the findings of [15] and [12].

It is remarkable that the difference in HCT between the two HBMs (with consistent postures) was smaller (0.3-2.8 ms) than the difference caused by differing initial postures.

Definition of other Simulation Settings

The sensitivity study shows that the friction between the HBM and the vehicle is influencing the kinematics. A higher coefficient of friction leads to a smaller HCT and to a lower head impact point. To make simulations comparable it is important to fix the contact settings. In the literature, coefficients of friction up to 0.5 are used [11, 12]. The friction in real life depends on the clothes worn by the pedestrian and the vehicle surface. For the procedure, however, the friction has to be harmonised and it was decided to use a coefficient of friction of 0.3, which is in agreement with several other studies [34, 42–46]. Elliott et al. [46] showed that for MADYMO models a friction coefficient of 0.3 led to the best correlation with PMHS tests of [19].

The implemented contact algorithms in different codes are varying. It was observed that changing the penalty formulation causes higher differences in HCT than using the other HBM model. Therefore, consistent contact formulations have to be applied in other codes.

The impact with the family car at 40 km/h was simulated with and without pre-simulations for the GHBMC and THUMS models, for establishing the equilibrium and the ground force. The skin of the pedestrian models was switched to rigid and gravity was applied until the contact force with the ground equalled the weight force of the HBM. No significant effect on the kinematics was observed. For studies focusing on injury mechanisms, e.g. knee ligament rupture, however, it might be important to consider the loading due to the body weight, but for the kinematics the effect seems to be negligible.

The sensitivity study shows that trajectories are relatively steady, while head impact time is sensitive to minor changes of the boundary conditions. This is critical, as there have been already simulations reported to Euro NCAP in which the time needed for the system to fully deploy was practically identical to the head contact time. Therefore, small tolerances of this output measure would be desirable for the certification of HBMs, which seems to be challenging based on the results of the current study.

Final Procedure

It has been feasible to apply the developed procedure to the two HBMs without major problems. All load cases led to plausible results and no obvious unrealistic behaviour of the HBMs or the GV models was observed. The differences in terms of the response trajectories between the two models became smaller with higher impact velocities.

Surprisingly, in most cases where significant differences in HCT were found, only small deviations in the trajectories were observed, i.e., for SUV impact at 40 km/h, the difference in the end position of HCT was 112 mm, which is only 2% of the path length. Even for the simulation with the highest difference at the time of the head impact, the difference was only 4 % of the path length, which is small compared to the 15% of the path length corridor proposed in [47].

The knee trajectories showed the biggest differences between the two models. This was also observed when using an alternative tracking point instead of the centre of the patella (midpoint of lateral and medial femoral epicondyle). Differences of the knee kinematics might be caused by the anthropometric differences of the two models (the femur is 25 mm longer in the GHBMC than in the THUMS). As the knee kinematics have little importance for the assessment of deployable systems, the corridors for this tracking point could be excluded.

Some stability problems and numerical issues (hourglassing) of the models were identified in the study and needed to be addressed, especially for the impact at 50 km/h (for the GHBMC the element form of the solid sections of the leg and torso flesh was changed to 2 and in THUMS the material type of the knee ligament tissue was modified to *MAT_PIECEWISE_LINEAR_PLASTICITY). This might have happened as validations are usually

performed at an impact velocity of 40 km/h. Hence, the procedure developed could also be applied by HBM developers to investigate the robustness of the models.

The study focused on only these simulation outputs relevant to the Euro NCAP assessment of deployable systems only. To date, no loads or injury criteria have been compared, yet the methodology does not exclude this for future steps. The present procedure is not intended as a validation of the biofidelity of human body models. It shows solely that the simulations with the two HBMs used in this study lead to comparable results when standardised and consistent boundary conditions are applied. The consistency in the results of the two models has strengthened the confidence of the authors in both the human body models and the procedure they have developed.

Outlook

The GV models are getting translated to the other codes and will be publicly available. As a next step the procedure will be applied to more models in multiple FE codes. Eventually, corridors and tolerances will be developed based on that results. A protocol for the certification of pedestrian models will be published, defining the procedure shown in Fig. 25 in detail, as part of the Euro NCAP Pedestrian test and assessment procedures. This certification process is very similar to the practice established in physical crash dummies, where different suppliers are allowed to supply a H-III dummy, yet everyone must meet agreed certification corridors.

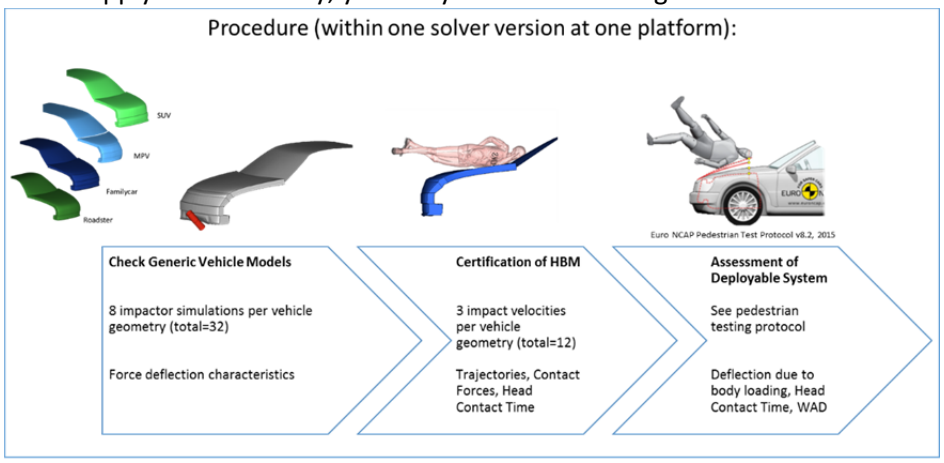

Fig. 25: Final procedure.

Prior to the HBM simulations a check of the GV models should be performed using the rigid impactor to ensure that the GV models always behave consistently (to avoid compatibility problems with future upcoming solver versions or very old versions). Within the certification simulations the presented will be applied to compare the response of the HBM which shall be used for the assessment simulations in the specific environment with the corridors derived from other HBMs applicable for the virtual testing.

A harmonised protocol for pedestrian simulations like proposed in the current paper will enable a comparable application of HBMs for virtual testing.

V. CONCLUSIONS

The study summarises the major boundary conditions affecting the HBM kinematics in pedestrian simulations and the following conclusions have been reached:

- The response of the generic vehicle model consisting of foams covered with interface layers was within the corridors derived from impactor simulations with full FE vehicles
- The importance of properly defined and specified boundary conditions for pedestrian impact simulations in order to gain comparable results was clearly demonstrated.
- While trajectories remained largely uninfluenced, the head contact time was sensitive to small changes of the initial posture.
- The posture of the arms, the height of the acetabulum and also the lateral distance between acetabulum and head COG affects HCT and caused differences of up to 5 ms.
- A variation of the friction between the HBM and the vehicle or a modification of the contact algorithm led to significant differences in terms of trajectories and HCT.

- The differences of HCT between the two HBMs were often smaller than the differences caused by a variation of boundary conditions.
- The differences of the final location of the tracking points between the two models were always higher than the difference caused by the variation of boundary conditions.
- The HCT of the two models was closer when the same boundary conditions were applied.
- The differences in the head trajectories of the two HBMs were generally low with a maximum difference of 4.13% of the path length at HCT.
- The simulations with two different state-of-the-art models in LS-DYNA led to very comparable results when the proposed procedure was applied.

The paper is listing relevant boundary conditions, which have to be considered when comparing simulation results with HBMs. A procedure representing all relevant load cases and defining all relevant boundary conditions was developed and was applied to two HBMs. The standardised procedure presented in the current paper can be applied to compare kinematics of new, updated or translated HBMs with other models.

VI. ACKNOWLEDGEMENT

The study is part of the CoHerent Project funded by Euro NCAP. The authors would like to thank ACEA TF-P (Belgium) for their support. Furthermore, we wish to thank the car manufactures for providing the data for the generic vehicles as well as for insightful discussions. The authors gratefully acknowledge the use of HPC resources provided by the ZID at Graz University of Technology, Austria.

The authors acknowledge that Elemance LLC (USA) is the exclusive distributor of the Global Human Body Model Consortium-owned GHBMC-Model and that Toyota Motor Corporation and Toyota Central R&D labs, Inc., (Japan) are the owners of the licensed Total Human Body Model for Safety.

VII. REFERENCES

1. Euro NCAP. "2016. "Euro NCAP Pedestrian Testing Protocol", Protocol 8.3,
2. Euro NCAP. "2015. "Pedestrian CAE Models & Codes", Technical Bulletin 13-v1,
3. Kitagawa Y, Yasuki T (2014) Development and Application of THUMS Version 4. *Proceedings of 5th International Symposium: Human Modeling and Simulation in Automotive Engineering,* 2014, Munich, Germany.
4. Watanabe R, Miyazaki H, Kitagawa Y, Yasuki T (2011) Research of the Relationship of Pedestrian Injury to Collision Speed, Car-type, Impact Location and Pedestrian Sizes Using Human FE Model (THUMS Version 4). *Proceedings of International Technical Conference on the Enhanced Safety of Vehicles,* 2011, Washington, D.C., USA.
5. Combest JC (2016) Current status and future plans of the GHBMC (Global Human Body Models Consortium). *Proceedings of 6th International Symposium: Human Modeling and Simulation in Automotive Engineering,* 2016, Heidelberg, Germany.
6. Untaroiu CD, Putnam JB, Schap J, Davis ML, Gayzik FS (2015) Development and Preliminary Validation of a 50th Percentile Pedestrian Finite Element Model. *Proceedings of IDETC/CIE 2015,* 2015, Boston, Massachusetts, USA.
7. Wu T, Kim T, Bollapragada V, Poulard D, Chen H, Panzer MB *et al.* (2017) Evaluation of biofidelity of THUMS pedestrian model under a whole-body impact conditions with a generic sedan buck. Traffic injury prevention, **18**(1)148-154.
8. Fuchs T, Fressmann D, Mayer C, Pipkorn B, Segura R, Weber J *et al. (*2014) Challenges in Using a Finite Element Human Body Model in Different Crash Codes. *Proceedings of IRCOBI Conference,* 2014, Berlin, Germany.
9. Ghosh P, Mayer C, Deck C, Bourdet N, Meyer F, Willinger R *et al. (*2016) Head Injury Risk Assessment in Pedestrian Impacts on Small Electric Vehicles using Coupled SUFEHM-THUMS Human Body Models Running in Different Crash Codes. *Proceedings of IRCOBI Conference,* 2016, Malaga, Spain.
10. Tang J, Zhou Q, Nie B, Yasuki T, Kitagawa Y. (2016) Influence of Pre-impact Pedestrian Posture on Lower Extremity Kinematics in Vehicle Collisions. SAE International Journal of Transportation Safety, **4**(2): pp.278–288.

11. Chen H, Poulard D, Crandall JR, Panzer MB (2015) Pedestrian Response with Different Initial Positions During Impact with a Mid-Sized Sedan. *Proceedings of International Technical Conference on the Enhanced Safety of Vehicles,* 2015, Gothenburg, Sweden.
12. Paas R, Östh J, Davidsson J (2015) Which Pragmatic Finite Element Human Body Model Scaling Technique Can Most Accurately Predict Head Impact Conditions in Pedestrian-Car Crashes? *Proceedings of IRCOBI Conference,* 2015, Lyon, France.
13. Kam CY, Kerrigan J, Meissner M, Drinkwater C, Murphy D, Bolton J *et al. (*2005) Design of a Full-Scale Impact System for Analysis of Vehicle Pedestrian Collisions. *Proceedings of SAE 2005 World Congress & Exhibition,* 2005, Detroit, USA.
14. Elliott JR, Simms CK, Wood DP. (2012) Pedestrian head translation, rotation and impact velocity. Accident Analysis & Prevention, **45**(0): pp.342–353.
15. Kerrigan J, Arregui C, Crandall J (2009) Pedestrian Head Impact Dynamics: Comparison of Dummy and PMHS in Small Sedan and large SUV Impacts. *Proceedings of International Technical Conference on the Enhanced Safety of Vehicles,* 2009, Stuttgart, Germany.
16. Kerrigan JR, Crandall JR, Deng B. (2007) Pedestrian kinematic response to mid-sized vehicle impact. International Journal of Vehicle Safety, **2**(3): pp.221–240.
17. Bose D, Bhalla KS, Untaroiu CD, Ivarsson BJ, Crandall JR, Hurwitz S. (2008) Injury Tolerance and Moment Response of the Knee Joint to Combined Valgus Bending and Shear Loading. Journal of Biomechanical Engineering, **130**(3): pp.1–8.
18. Rohlmann A, Neller S, Claes L, Bergmann G, Wilke HJ. (2001) Influence of a follower load on intradiscal pressure and intersegmental rotation of the lumbar spine. Spine, **26**(24): pp.557–561.
19. Subit D, Kerrigan J, Crandall J, Fukuyama K, Yamazaki K, Kamiji K *et al. (*2008) Pedestrian-vehicle interaction: Kinematics and injury analysis of four full-scale tests. *Proceedings of IRCOBI Conference,* 2008, Bern, Switzerland.
20. Schroeder G, Fukuyama K, Yamazaki K, Kamiji K, Yasuki T (2008) Injury mechanism of pedestrians impact test with a sport-utility vehicle and mini-van. *Proceedings of IRCOBI Conference,* 2008, Bern, Switzerland.
21. Forman J, Joodaki H, Forghani A, O Riley P, Bollapragada V, Lessley D *et al. (*2015) Biofidelity Corridors for Whole-Body Pedestrian Impact with a Generic Buck. *Proceedings of IRCOBI Conference,* 2015, Lyon, France.
22. Forman JL, Joodaki H, Forghani A, Riley PO, Bollapragada V, Lessley DJ *et al.* (2015) Whole-body Response for Pedestrian Impact with a Generic Sedan Buck. Stapp Car Crash Journal, **59**: pp.401–444.
23. Bose D, Bhalla K, Rooij L, Millington S, Studley A, Crandall J. "2004. "Response of the Knee Joint to the Pedestrian Impact Loading Environment, Warrendale, PA.
24. Kajzer J, Schroeder G, Ishikawa H, Matsui Y, Bosch U (1997) Shearing and Bending Effects at the Knee Joint at High Speed Lateral Loading. *Proceedings of 41st Stapp Car Crash Conference,* 1997.
25. Demetropoulos CK, Yang KH, Grimm MJ, Khalil TB, King AI (1998) Mechanical Properties of the Cadaveric and Hybrid III Lumbar Spines. *Proceedings of Stapp Car Crash Conference,* 1998.
26. SAE International. "2010. "Performance Specifications for a Midsize Male Pedestrian Research Dummy", Standard J2782-v201010, USA.
27. Untaroiu CD, Meissner MU, Crandall JR, Takahashi Y, Okamoto M, Ito O. (2009) Crash reconstruction of pedestrian accidents using optimization techniques. International Journal of Impact Engineering, **36**(2): pp.210–219.
28. Perry J. "1992. "Gait analysis", *Slack Incorporated.*
29. Euro NCAP. "2015. "AEB VRU systems", Test Protocol-v1,
30. Wu G, Siegler S, Allard P, Kirtley C, Leardini A, Rosenbaum D *et al.* (2002) ISB recommendation on definitions of joint coordinate system of various joints for the reporting of human joint motion—part I: ankle, hip, and spine. Journal of biomechanics, **35**(4): pp.543–548.
31. Wu G, van der Helm, Frans C.T., Veeger H, Makhsous M, van Roy P, Anglin C *et al.* (2005) ISB recommendation on definitions of joint coordinate systems of various joints for the reporting of human joint motion—Part II. Journal of biomechanics, **38**(5): pp.981–992.
32. Martinez L, Guerra LJ, Ferichola G, Garcia A, Yang J (2007) Stiffness corridors of the European fleet for pedestrian simulation. *Proceedings of International Technical Conference on the Enhanced Safety of Vehicles,* 2007.
33. Isshiki T, Konosu A, Takahashi Y (2014) Development of an Appropriate Pedestrian Legform Impact Test Method which can be used for all Types of Vehicles including High Bumper Vehicles. *Proceedings of IRCOBI Conference,* 2014, Berlin, Germany.

34. Li G, Yang J, Simms C. (2015) The influence of gait stance on pedestrian lower limb injury risk. Accident Analysis & Prevention, **85**: pp.83–92.
35. Soni A, Robert T, Rongieras F, Beillas P. (2013) Observations on pedestrian pre-crash reactions during simulated accidents. Stapp Car Crash Journal, **57**: pp.157–183.
36. PIPER. "Position and Personalize Advanced Human Body Models for Injury Prediction", http://www.piper-project.eu/ [Accessed 26 May 2017].
37. Schroeder G, Konosu A, Ishikawa H, Kajzer J (2000) Injury Mechanism of Pedestrians during a Front- End Collision with a Late Model Car*. Proceedings of JSAE Spring Forum for Pedestrian Protection,* 2000, Yokohama, Japan.
38. Brun-Cassan F, Vincent JC, Tarriere C, Fayon A, Cesari D, Cavallero C *et al. (*1984) Comparison of Experimental Car-Pedestrian Collisions Performed with Various Modified Side-Impact Dummies and Cadavers*. Proceedings of 28th Stapp Car Crash Conference,* 1984, Chicago, USA.
39. Crandall J, Wiley K, Longhitano D, Akiyama A (2005) Development of performance specifications for a pedestrian research dummy*. Proceedings of International Technical Conference on the Enhanced Safety of Vehicles,* 2005.
40. Coley G, Lange R de, Oliveira P de, Neal-Sturgess CE, Happee R (2001) Pedestrian human body validation using detailed real-world accidents*. Proceedings of IRCOBI Conference,* 2001.
41. Paas R, Masson C, Davidsson J. (2015) Head boundary conditions in pedestrian crashes with passenger cars. International Journal of Crashworthiness, **20**(6): pp.547–559.
42. Simms C, Wood DP. (2006) Pedestrian Risk from Cars and Sport Utility Vehicles - A Comparative Analytical Study. Proceedings of the Institution of Mechanical Engineers, Part D: Journal of Automobile Engineering, **220**(8): pp.1085–1100.
43. Crocetta G, Piantini S, Pierini M, Simms C. (2015) The influence of vehicle front-end design on pedestrian ground impact. Accident Analysis & Prevention, **79**: pp.56–69.
44. Mizuno Y, Ishikawa H (2001) Summary of IHRA Pedestrian Safety WG Activities – Proposed Test Methods to Evaluate Pedestrian Protection Aforded by Passenger Cars*. Proceedings of International Technical Conference on the Enhanced Safety of Vehicles,* 2001.
45. Fahlstedt M, Halldin P, Kleiven S. (2016) Comparison of multibody and finite element human body models in pedestrian accidents with the focus on head kinematics. Traffic injury prevention, **17**(3): pp.320–327.
46. Elliott J, Lyons M, Kerrigan J, Wood D, Simms C. (2012) Predictive capabilities of the MADYMO multibody pedestrian model. Proceedings of the Institution of Mechanical Engineers, Part K: Journal of Multi-body Dynamics, **226**(3): pp.266–277.
47. SAE International. "2010. "Pedestrian Dummy Full Scale Test Results and Resource Materials", Standard J2868-v201010, USA.

VIII. APPENDIX

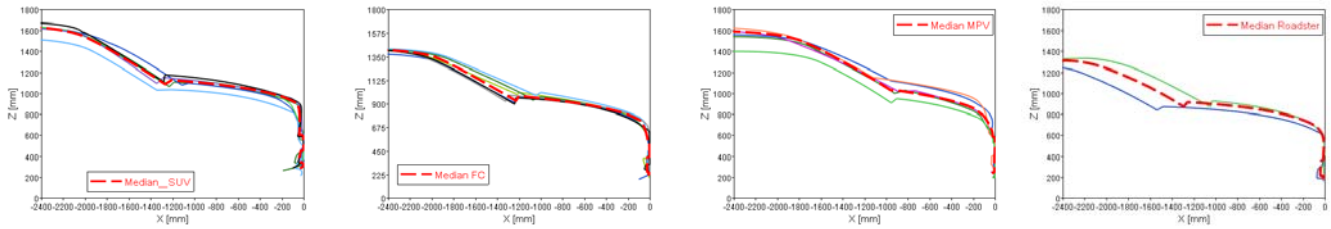

Fig. A1. Comparison of vehicle geometries (median versus vehicle shapes of current European fleet).

TABLE AI
GENERIC FAMILYCAR MODEL

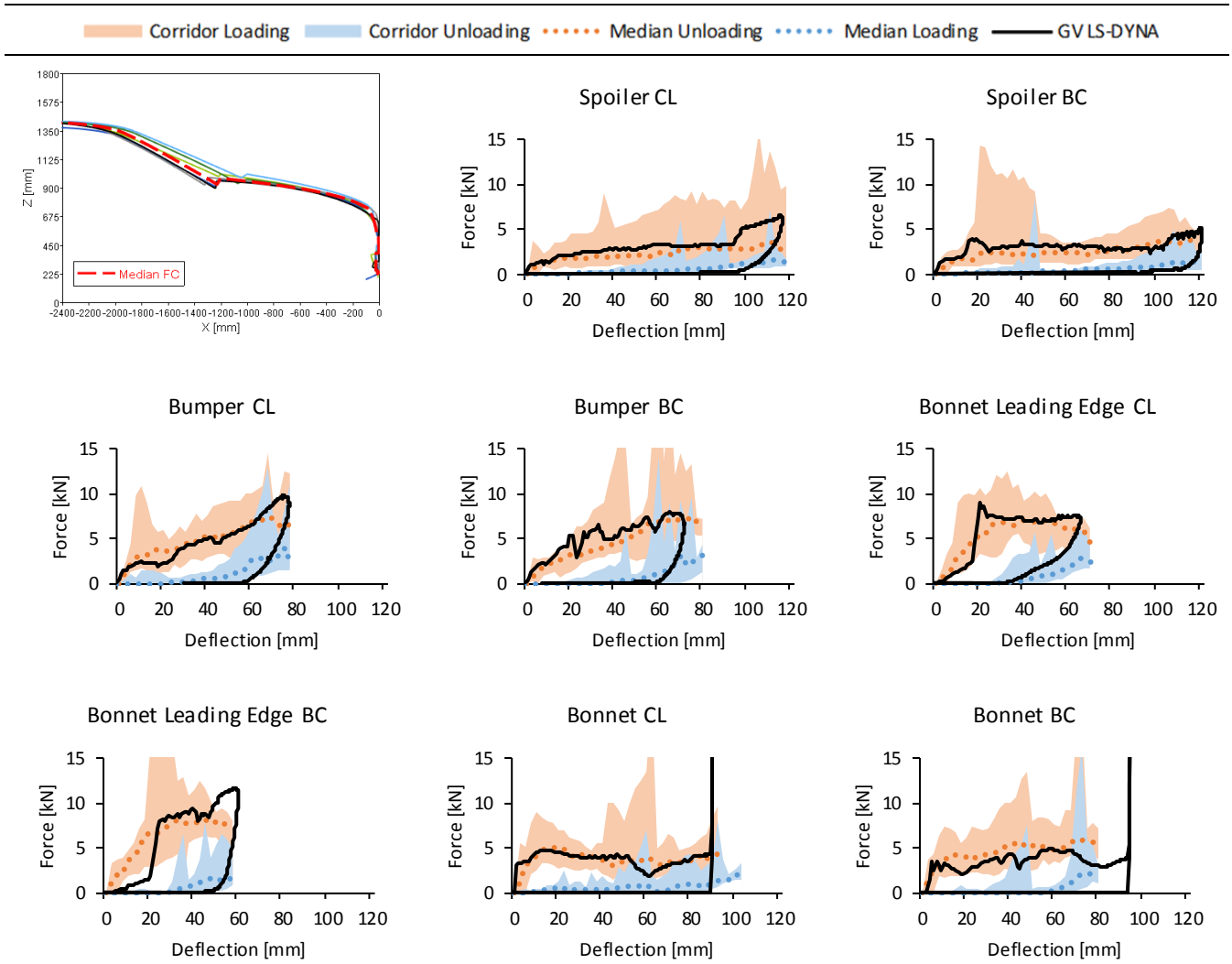

TABLE AII
GENERIC MPV MODEL

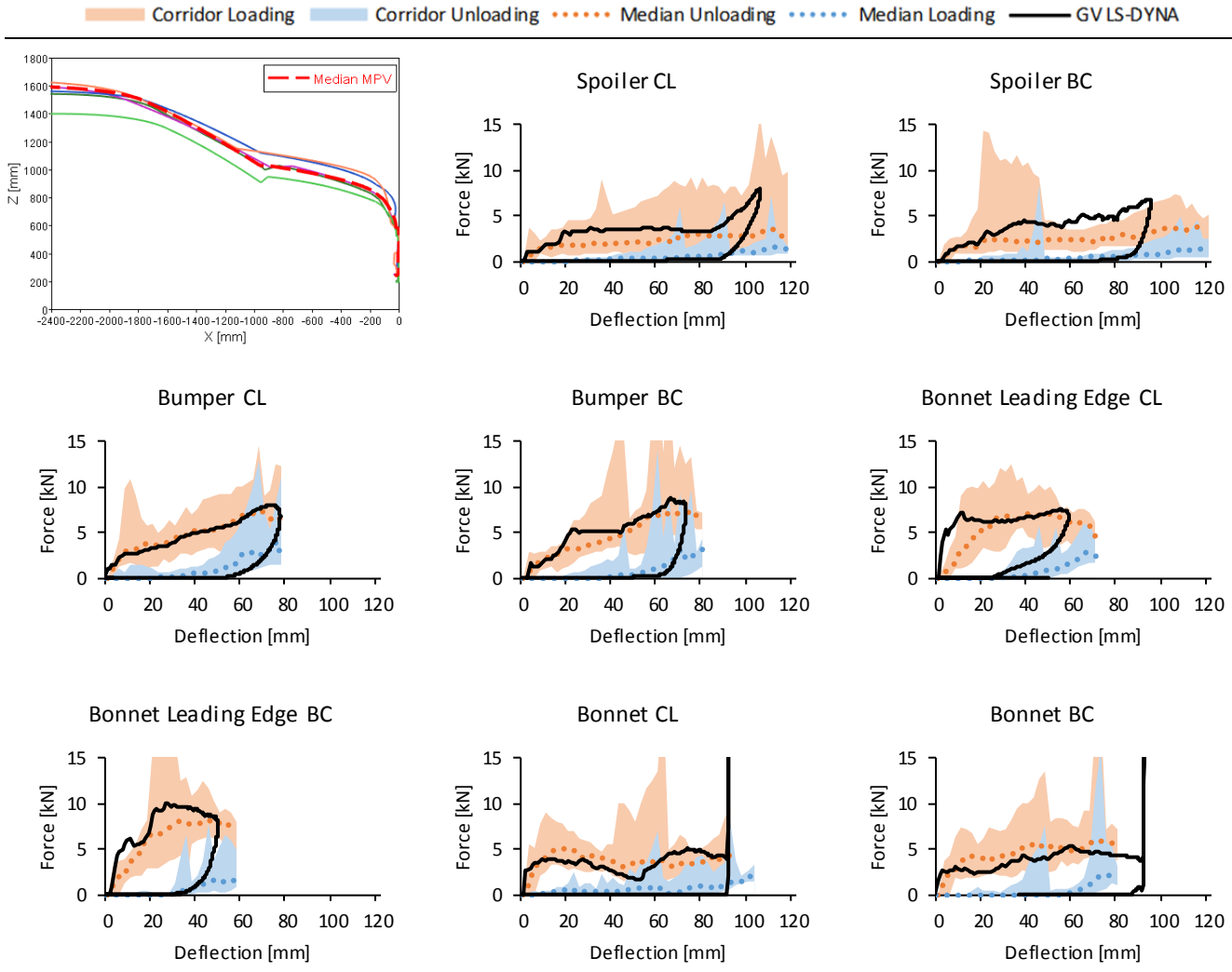

TABLE AIII
GENERIC ROADSTER MODEL

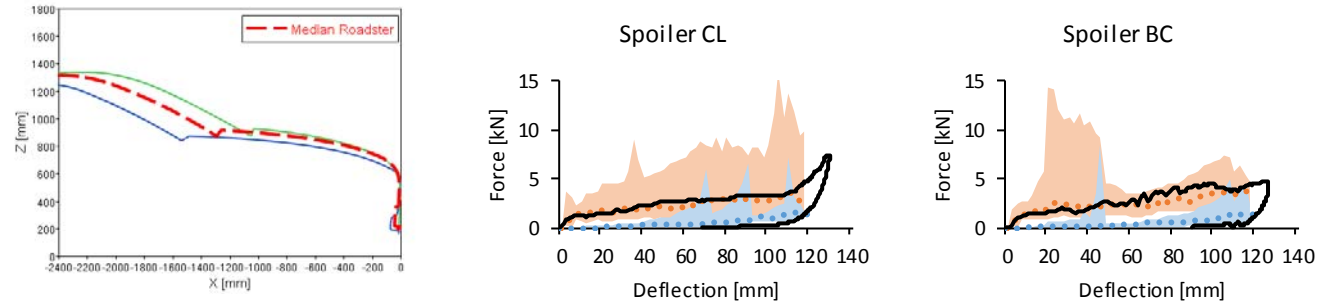

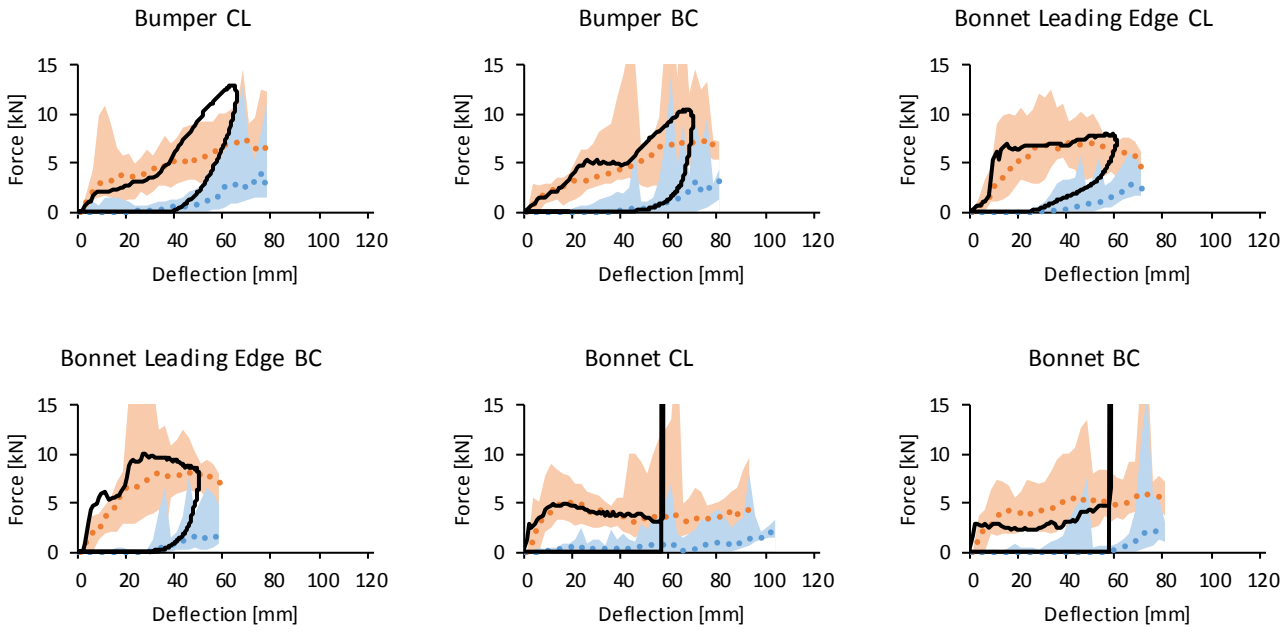

TABLE AIV
GENERIC SUV MODEL

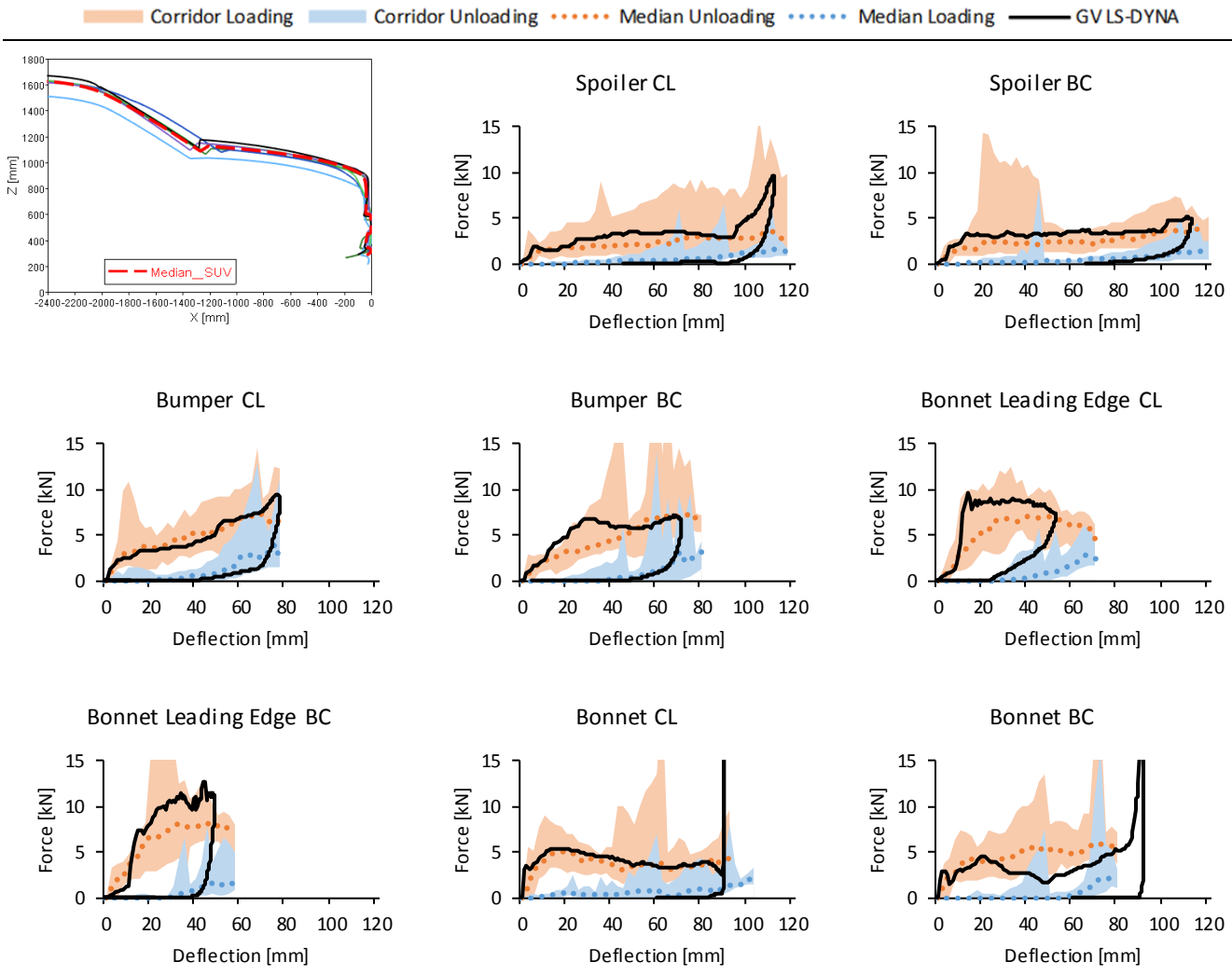

TABLE AIV
PARAMETER SETS FOR GENERIC VEHICLE MODELS

Parameter	Abbr.	Spoiler	Bumper	Grill	Bonnet lead	Bonnet
density foam	RO	7.000E-08	7.000E-08	7.000E-08	7.000E-08	2.000E-09
thickness interface layer	TH	1.680E+00	1.860E+00	1.990E+00	1.000E+00	1.300E+00
Thickness of the wrapping rear interface layer	RTH	1.700E+00	-	-	1.400E-01	-
Thickness of the wrapping front interface layer	FTH	1.000E+00	-	-	-	2.000E-01
Thickness of the wrapping side interface layer	STH	-	-	-	-	4.000E-01
Material ID Interface layer	MT	9900004	9900004		9900004	9900002
Primary Stiffness	T1	2.899E-05	6.337E-05	3.270E-06	8.000E-03	1.225E-09
Secondary Stiffness	T2	1.382E-05	7.743E-05	3.646E-03	1.000E-17	1.225E-09
Tertiary Stiffness	T3	2.997E-02	5.127E-04	1.466E-03	1.000E-17	1.225E-09
(Yield) Strain at transition between primary and secondary stiffness	E1	1.002E-04	2.999E-01	3.203E-01	1.000E-02	2.986E-01
Transition Stiffness between yield and compaction stiffness	E2	4.877E-01	8.497E-01	8.221E-01	5.100E-01	8.000E-01
Energy Absorption	AB	9.500E-01	9.500E-01	9.500E-01	9.500E-01	9.500E-01
Offset between interface and compaction layer	OF	198	99	99	99	99 (RDS=64)

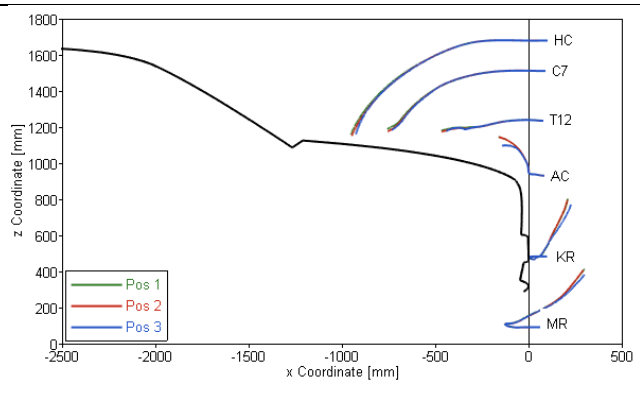

Fig. A2. Influence of initial arm posture on trajectories

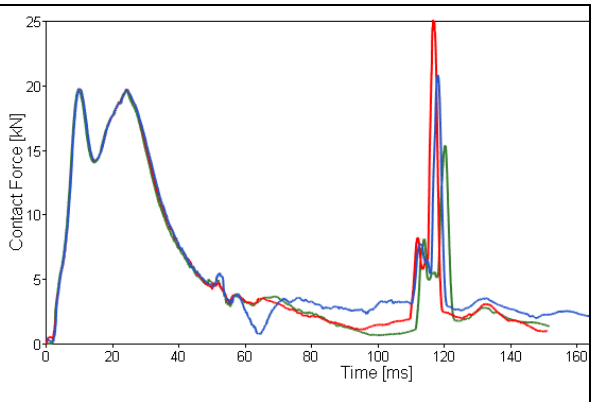

Fig. A3. Influence of initial arm posture on total

(impact of THUMS with generic SUV model at 40 km/h)	contact forces. (impact of THUMS with generic SUV model at 40 km/h)

TABLE AV:
RESULTS OF THUMS AND GHBMC SIMULATIONS

Simulation	*Contact Forces*	*Trajectory*	*HCT [ms]*
FC 30 km/h	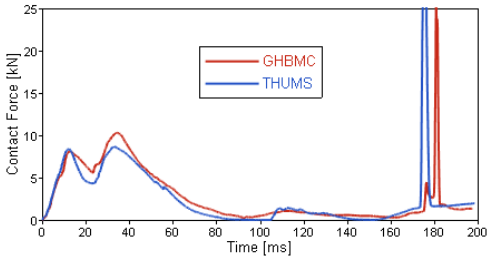	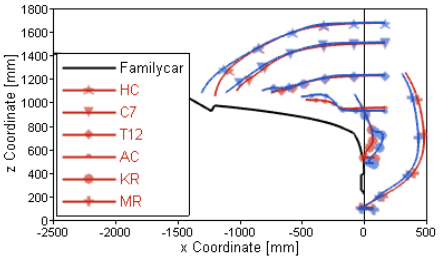	*173.3* *174.9* *ΔHCT=1.6*
FC 40 km/h	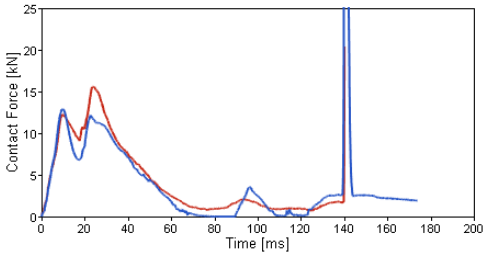	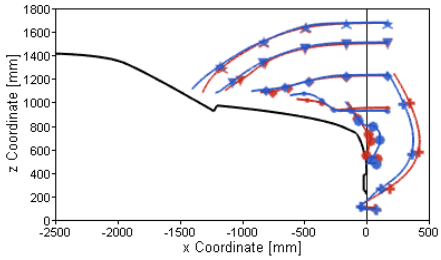	139.0 139.7 ΔHCT=0.7
FC 50 km/h	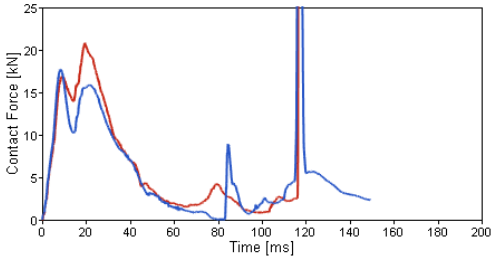	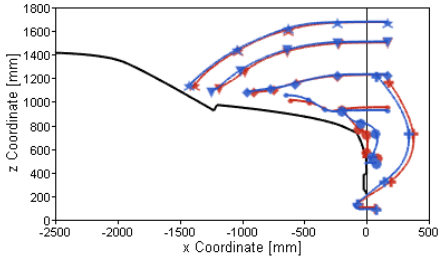	115.0 115.9 ΔHCT=0.9
MPV 30 km/h	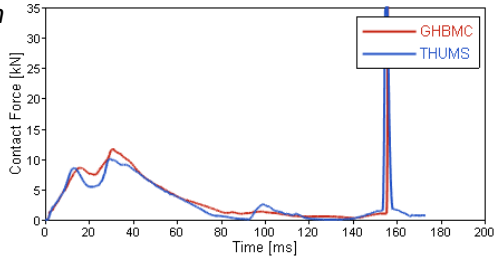	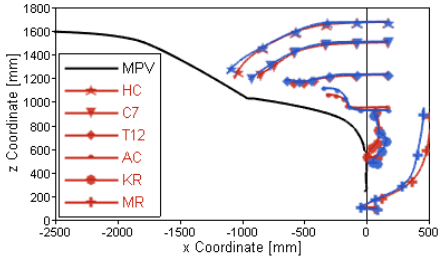	152.5 154.4 ΔHCT=1.9
MPV 40 km/h	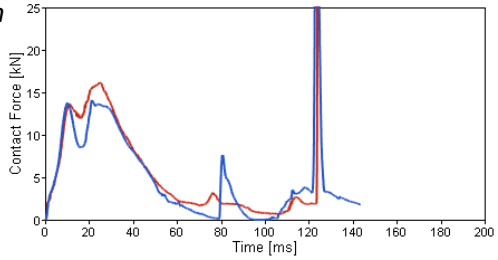	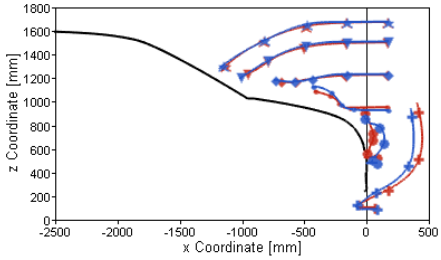	121.4 123.2 ΔHCT=1.8
MPV 50 km/h	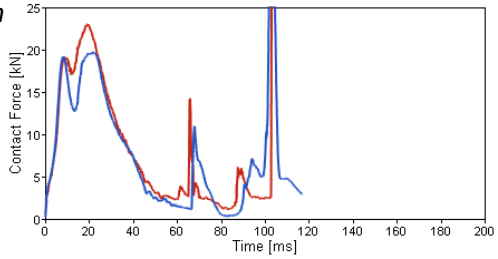	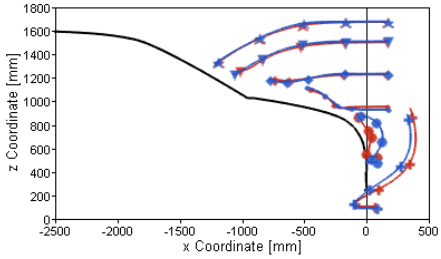	100.6 102.9 ΔHCT=2.3

RDS 30 km/h

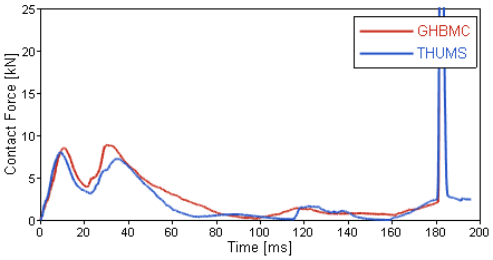

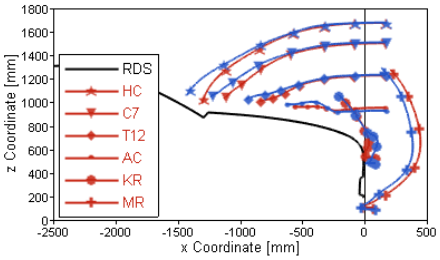

180.2
180.8
ΔHCT=0.6

RDS 40 km/h

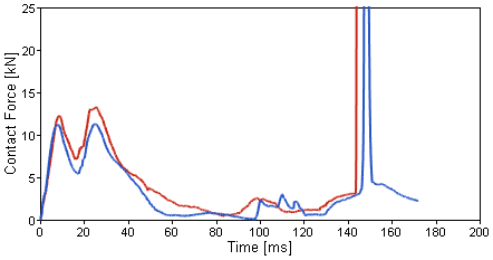

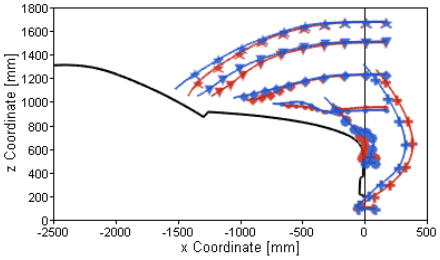

146.2
143.4
ΔHCT=2.8

RDS 50 km/h

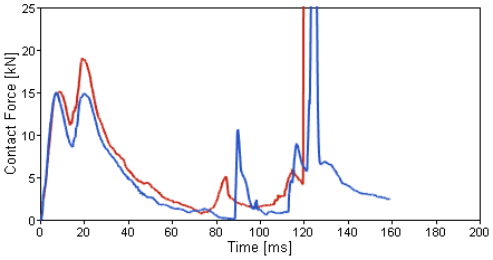

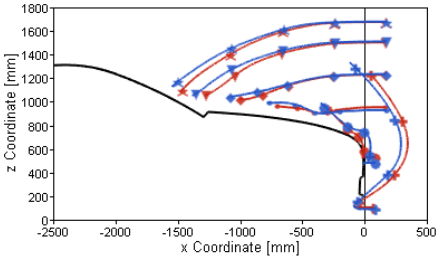

121.6
118.9
ΔHCT=2.7

SUV 30 km/h

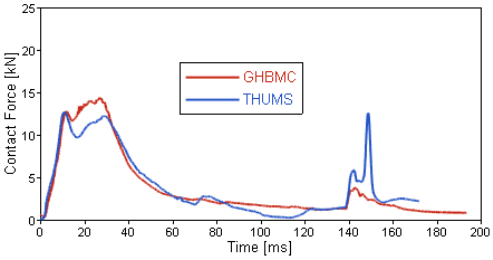

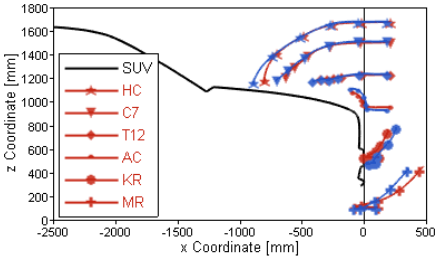

137.4
136.6
ΔHCT=0.8

SUV 40 km/h

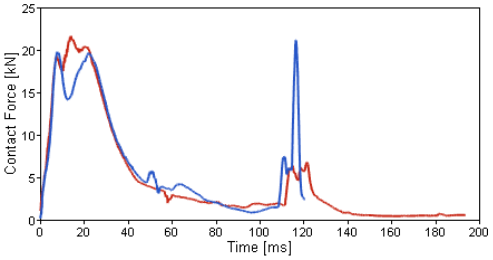

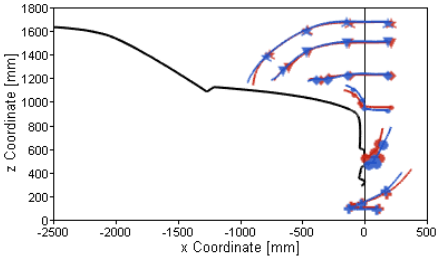

108.8
111.6
ΔHCT=2.8

SUV 50 km/h

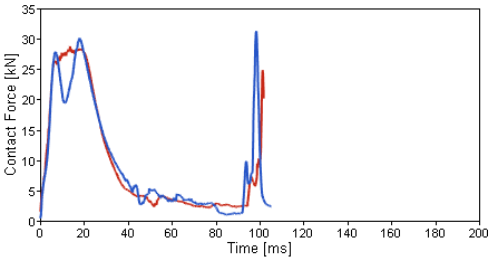

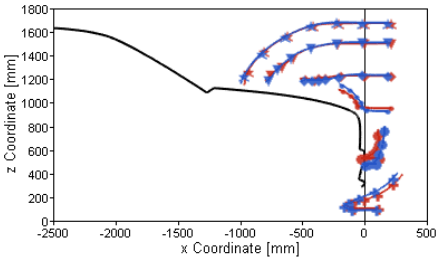

92
94.2
ΔHCT=2.2

TABLE AVI
INITIAL POSTURES

		THUMS											GHBMC		
		Pos 1	Pos 2	Pos 3	Pos 4	Pos 5	Pos 6	Pos 7	Pos 8	Pos 9	Pos 10	Pos 11	Pos 1	Pos 2	Pos 3
Heel to heel distance (x)	P	316	316	316	313	316	316	**326**	**333**	311	316	316	314	314	314
Height of AC relative to the ground level	AC_z	931	931	931	931	931	931	**946**	**946**	931	931	931	956	956	956
Right Upper Leg Angle (Y with respect to horizontal)	K	87	87	87	**85**	87	87	87	87	**85**	87	87	87	87	87
Left Upper Leg Angle (Y with respect to the horizontal)	M	103	103	103	**109**	103	103	103	103	**108**	103	103	103	103	103
Right Knee flexion Angle	G	166	166	166	**168**	166	166	166	166	**168**	166	166	166	166	166
Left Knee flexion Angle	H	177	177	177	**161**	177	177	177	177	**162**	177	177	177	177	177
Distance between right heel and AC (X)	PR_x	216	216	216	**239**	216	216	216	223	**242**	216	216	215	215	215
Right Upper Arm Angle (Y with respect to horizontal)	T	**97**	106	**98**	108	*106*	*106*	*106*	**98**	**96**	**100**	*106*	**95**	**109**	**98**
Left Upper Arm Angle (Y with respect to horizontal)	U	**96**	65	**70**	62	65	65	65	**70**	**74**	**60**	64	**85**	**59**	**69**
Right Elbow flexion Angle	V	**129**	152	**144**	**177**	152	152	152	**144**	**141**	**145**	152	**116**	**152**	**136**
Left Elbow flexion Angle Left	W	**137**	151	**162**	**152**	151	151	151	**162**	**170**	**148**	151	**125**	**155**	**166**
x-Position of HC relative to AC	HC_x	48	47	48	**15**	**58**	**42**	47	48	**15**	**98**	**99**	41	41	41
Height of HC relative to the ground level	HC_z	1680	1681	1681	1681	1678	1682	**1696**	**1696**	1681	**1678**	**1665**	1678	1678	1678
x-Position of C7 relative to AC	C7x	6	5	6	**20**	6	5	5	6	**20**	**46**	8	7	7	7